



A Comparison Study of Multidirectional Waves Generated in Laboratory Basins

Miles, M.D.; Benoit, M.; Frigaard, Peter; Hawkes, P. J.; Schäffer, H. A.; Standsberg, C. T.

Published in:

Proceedings of the 27th IAHR Congress, San Francisco, 10-15 August 1997

Publication date:

1997

Document Version

Early version, also known as pre-print

[Link to publication from Aalborg University](#)

Citation for published version (APA):

Miles, M. D., Benoit, M., Frigaard, P., Hawkes, P. J., Schäffer, H. A., & Standsberg, C. T. (1997). A Comparison Study of Multidirectional Waves Generated in Laboratory Basins. In Mansard, Etienne (ed.) (Ed.), *Proceedings of the 27th IAHR Congress, San Francisco, 10-15 August 1997: IAHR Seminar : Multidirectional Waves and their Interaction with Structures* Canadian Government Publishing.

General rights

Copyright and moral rights for the publications made accessible in the public portal are retained by the authors and/or other copyright owners and it is a condition of accessing publications that users recognise and abide by the legal requirements associated with these rights.

- Users may download and print one copy of any publication from the public portal for the purpose of private study or research.
- You may not further distribute the material or use it for any profit-making activity or commercial gain
- You may freely distribute the URL identifying the publication in the public portal -

Take down policy

If you believe that this document breaches copyright please contact us at vbn@aub.aau.dk providing details, and we will remove access to the work immediately and investigate your claim.

A Comparison Study of Multidirectional Waves Generated in Laboratory Basins

M.D. MILES¹, M. BENOIT², P. FRIGAARD³,
P.J. HAWKES⁴, H.A. SCHÄFFER⁵ and C.T. STANSBERG⁶

¹ Canadian Hydraulics Centre, Ottawa, Canada

² Laboratoire National d'Hydraulique, Chatou, France

³ Aalborg University, Aalborg, Denmark

⁴ HR Wallingford, Oxfordshire, UK

⁵ Danish Hydraulic Institute, Hørsholm, Denmark

⁶ Marintek, Trondheim, Norway

Abstract

This paper describes the results of a comparison study that was carried out by the IAHR working group on multidirectional waves. Multidirectional waves were generated in six different laboratory basins according to specified target directional wave spectra for both broad and narrow spreading functions. The measured waves were then analysed by a common MEM (maximum entropy) method to investigate the variability due to different wave synthesis and generation methods. Numerical simulations were also performed to evaluate the effects of wave diffraction and reflection.

1 Introduction

Due to increasing interest in the use of multidirectional waves for physical model tests in hydraulics laboratories, the Maritime Hydraulics Section of the IAHR formed a working group on multidirectional waves in 1994 (Briggs, 1997). Two of the tasks carried out by this working group were comparison studies of the generation and analysis methods that are typically used for the reproduction and measurement of multidirectional wave fields in laboratory basins using segmented wave machines. The first study (Hawkes et al., 1997) compared the results of different wave analysis methods on common sets of synthesized and measured directional wave data. This paper presents the results of the second study which used a common analysis method to compare multidirectional waves that were generated and measured in several different laboratory basins.

The total variability depends on numerous factors associated with the different wave generation methods. Due to the expense of conducting tests in multidirectional wave basins and the limited number of participating laboratories, the physical wave tests could provide useful information on the overall variability but could not be used to assess the relative influence of individual factors. Consequently, it was decided to also carry out some numerical modelling of a typical wave basin equipped with a segmented wave generator. Since certain individual factors could be easily controlled in the numerical model, it was used to assess the relative influence of factors such as wave diffraction and reflection in the basin. The numerical model results would also be useful for interpreting the results from the physical wave generation tests.

2 Wave Synthesis and Generation Methods

Sand and Mynett (1987) contains a very good overview of the synthesis and generation methods that are typically used to produce multidirectional waves in laboratory basins. Wave synthesis generally consists of defining a pseudo-random wave field of specified duration that represents a particular realization of a natural sea state defined by a given directional spectrum, $S(f, \theta)$. The resulting wave field usually consists of the superposition of several hundred or several thousand sinusoidal wave components with individual amplitudes, phases and directions of propagation set according to a particular wave synthesis model.

The two most commonly used synthesis models are the double summation model and the single summation model. The double summation model contains wave components with many different directions at each frequency whereas the single summation model has only one wave direction at each frequency. The main advantage of the single summation model is that the resulting wave field is spatially homogeneous for the durations that are typically used for model tests. In contrast, the double summation model only becomes spatially homogeneous for very long record durations. The relative merits of the single and double summation models are discussed in Jefferys (1987) and Miles and Funke (1989). These two basic synthesis models can also be implemented in several different ways. For example, the discrete frequencies can either be uniformly spaced for FFT operations or non-harmonic frequencies can be used. One example of the non-harmonic approach is the equal energy method in which the spectrum is divided into bands of equal energy and each band is represented by sinusoidal components of equal amplitude with random phase angles. In the harmonic approach, the amplitudes and phases of the sinusoidal components can either be set by the random phase method or by the random Fourier coefficient method. Similarly, the discrete wave angles can either be uniformly spaced or selected at random according to the cumulative distribution of the target spreading function. Thus, when comparing multidirectional waves generated in different laboratory basins, a certain degree of variability can

Differences in these various wave generation methods and procedures for dealing with constraints will also contribute to the variability when a given directional spectrum is generated in different laboratory basins.

3 Test Cases

Six test cases were selected based on the primary tests cases A1 and B1 that were used for the companion comparison study of directional wave analysis methods (Hawkes et al., 1997). The various parameters for these test cases are listed in Table 1 where s and θ_0 are the parameters of the following target directional spreading function:

$$D(\theta) = \frac{\Gamma(s+1)}{2\sqrt{\pi}\Gamma(s+0.5)} \cos^{2s}((\theta - \theta_0)/2) \quad (1)$$

In Table 1, d is the water depth and x_c is the distance from the centre wave probe to the wave generator. The target spectrum for all cases is a JONSWAP with $\gamma = 3.3$.

Test	T_p	H_{m0}	θ_0	s	d	x_c	Comments
P1	1.8 s	12 cm	0°	6	3.0 m	8.0 m	Standard test, deep water
P2	1.8 s	6 cm	0°	6	0.5 m	3.0 m	Standard test, shallow water
Q1	1.8 s	12 cm	0°	40	3.0 m	8.0 m	Narrow spread, deep water
Q2	1.8 s	6 cm	0°	40	0.5 m	3.0 m	Narrow spread, shallow water
R1	1.8 s	24 cm	0°	6	3.0 m	8.0 m	Larger amplitude, deep water
R2	1.8 s	12 cm	0°	6	0.5 m	3.0 m	Larger amplitude, shallow water

Table 1: Test cases for multidirectional waves to be generated in laboratory basins

Two versions of each of the three primary P, Q and R cases were defined for depths of 0.5 m and 3.0 m because most of the available basins were restricted to either deep or shallow water. The wave amplitudes for cases P and Q were chosen to be within the linear range. Case R is case P with the wave height doubled to investigate the effects of increased wave steepness.

A standard sensor configuration was specified for measuring the waves generated in each basin. This consisted of a symmetric array of 6 wave elevation probes with an optional 2-axis current meter, as shown in Figure 1. The current meter measured the horizontal velocity components u and v at the same (x, y) position as wave probe 6. This sensor configuration is the same as that used in the companion study on wave analysis methods and allows the directional spectra to be estimated either

In addition to the spreading function $D(f, \theta)$, MEMVL and MEMWP also compute the mean wave direction $\theta_m(f)$ and the spreading width $\sigma_\theta(f)$ for the main incident wave field by integrating over an angular range from $\theta_p - \pi/2$ to $\theta_p + \pi/2$ where $\theta_p(f)$ is the wave angle corresponding to the main peak of $D(f, \theta)$. This procedure is used to minimize the effects of any reflected waves in the basin on the estimates of $\theta_m(f)$ and $\sigma_\theta(f)$ for the main incident wave system.

5 Numerical Simulations

Some numerical simulations were first carried out using the CHC WAGEN5 numerical model. WAGEN5 is an extended version of the WAGEN linear boundary element diffraction model described in Isaacson and Mathai (1993). It can be used to predict the wave fields produced by one or more segmented wave generators in a basin of constant depth. The basin may also contain any combination of fully reflecting walls or partially reflecting passive wave absorbers. The wave generators can also be modelled either with or without active wave absorption capability. The WAGEN numerical model, upon which WAGEN5 is based, has been previously verified by wave basin experiments (Hiraishi et al., 1992).

WAGEN5 was used to simulate the waves produced in a typical 20 m by 30 m wave basin with a 60-segment wave generator installed along one 30 m side and passive absorbers installed on the other three sides. The target wave field was first synthesized by the single summation method with random wave angles and the corresponding wave machine paddle motions were calculated by the standard Snake Principle method. The WAGEN5 numerical model was then used with linear superposition to compute the irregular multidirectional wave field that would be produced in the basin by these paddle motions. The effects of wave diffraction and reflection could be studied independently by specifying different reflection coefficients for the passive absorbers in the simulations.

Numerical simulations were run for test cases P1 and Q1 with a water depth of 3.0 m. Since WAGEN5 is a linear model, it was not necessary to run a separate simulation for test case R1 because the results would be the same as case P1. In each case, the synthesized waves had 2048 Fourier components with random phases and directions to obtain a non-repetitive duration of 1500 seconds at a frequency resolution of 0.0006667 Hz.

The maximum wave angle that can be generated by a segmented machine installed on one side of a basin is limited by geometrical constraints. The theoretical spreading functions were truncated at ± 70 deg. and re-normalized to comply with this constraint. In test case P1, this truncation resulted in a target spreading width of $\sigma_\theta = 29.5$ deg. which is slightly less than the theoretical value of $\sigma_\theta = 31.7$ deg. for the original spreading function. Due to the narrower spreading, this truncation had no significant effect on test case Q1.

cases shown in Figure 4, the σ_θ values in the vicinity of point A are quite close to the target values of 29.5 and 12.7 degrees for test cases P1 and Q1, respectively.

Time series data were also generated from the numerical simulations for the wave sensor configuration shown in Figure 1 with the centre wave probe (no. 6) and the (u, v) current meter located at point A in the basin. These time series data were then processed by the same MEMVL and MEMWP programs that were used to analyze the measured data from the laboratory basin tests, as described in Section 6. The time series records were 1500 seconds long and the MEM analysis was performed at a frequency resolution of 0.04 Hz. The following three sets of time series data were analyzed for each of the P1 and Q1 test cases:

SYN	The wave field synthesized by the single summation method with random wave angles for the target directional spectrum. This synthesized wave field is homogeneous over the entire (x, y) plane and is not related to any particular basin.
GEN1	The generated wave field at point A in the 20 by 30 m basin as computed by the numerical model for the case of a 60-segment wave generator on one side and perfect wave absorbers ($C_R = 0.0$) on the other 3 sides.
GEN2	The generated wave field at point A in the 20 by 30 m basin as computed by the numerical model for the case of a 60-segment wave generator on one side and partially reflecting wave absorbers ($C_R = 0.2$) on the other 3 sides.

The resulting $D(\theta)$ spreading functions from the MEM analysis of these data sets for test cases P1 and Q1 are shown in Figures 5 and 6. These plots show the spreading function $D(f, \theta)$ at $f = f_p$ and the average spreading function computed as follows:

$$\text{Average } D(\theta) = \frac{\int_{f_1}^{f_2} S_\eta(f) \cdot D(f, \theta) df}{\int_{f_1}^{f_2} S_\eta(f) df} \quad (2)$$

where $f_1 = 0.4$ Hz and $f_2 = 1.0$ Hz.

It can be seen in Figure 5 that the SYN and GEN1 spreading functions are almost identical in all cases so wave diffraction has very little effect at point A. The GEN2 spreading functions have a slightly narrower main peak and broad secondary peak at 180 deg. due to the reflected waves. The average SYN $D(\theta)$ matches the target spreading function very closely for the (η, u, v) data but is slightly narrower than the target for 6 probe array data.

The average SYN and GEN1 $D(\theta)$ results for case Q1 also match the target spreading function very closely, as shown in Figure 6. As expected, the GEN2

Laboratory	Water Depth	Cases Performed	η, u, v data	6-probe array
Lab 1	0.5 m	P2, Q2, R2	yes	yes
Lab 2	3.0 m	P1, Q1, R1	yes	yes
Lab 3	0.5 m	P2, Q2, R2	no	yes
Lab 4	0.5 m	P2, Q2, R2	yes	yes
Lab 5	3.0 m	P1, Q1, R1	no	yes
Lab 6	0.5 m	P2, Q2, R2	no	yes

Table 2: Test cases performed at each laboratory

Since the objective was to investigate overall variability without regard to individual basins, the various sets of wave data have been given designations of Lab 1 to Lab 6 with the numbers 1 to 6 assigned in no particular order. The lab numbers used in this paper also have no particular correspondence to those in Hawkes et al. (1997).

The test cases performed at each laboratory are listed in Table 2. The waves were synthesized and generated by the standard operational methods normally used in each laboratory. The waves were then measured using the standard instrumentation in each laboratory with the various wave sensors configured as shown in Figure 1. Data were collected from each sensor at a 20 Hz sampling rate for a duration of 1500 seconds. The resulting time series data were then sent to the Canadian Hydraulics Centre for analysis by the MEMVL and MEMWP programs described in Section 4. The directional wave analysis was carried out at a frequency resolution of 0.04 Hz.

Since only six sets of data were available, it was not possible to evaluate the effects of different water depths. Consequently, the data from the six test cases P1, P2, Q1, Q2, R1 and R2 have been merged into three test cases designated P, Q and R for the purpose of comparing results from the various laboratory basins.

After performing the directional analysis, it was also discovered that the Lab 3 waves had not been generated for the correct target spreading functions. A target spreading function of the form $\cos^n(\theta)$ had been used with n values of 6 and 40 instead of the specified $\cos^{2s}(\theta/2)$ spreading function with s values of 6 and 40. Consequently, the target σ_θ values for the Lab 3 waves were actually 21.6 deg. for test cases P and R and 9.0 deg. for test case Q instead of the specified values of 31.7 deg. for cases P and R and 12.7 deg. for case Q. The target θ_m values for the Lab 3 data were correct. Unfortunately, it was not possible to schedule the Lab 3 basin to repeat the tests with the correct target spreading functions. Since only six sets of data were available for this comparison study, it was decided to retain the Lab 3 results as much as possible while noting the different target spreading widths that had been used to generate these particular waves.

The mean wave direction $\theta_m(f)$ and the spreading width $\sigma_\theta(f)$ are plotted as functions of frequency for Test Case P in Figure 12. The target frequency spectrum $S_\eta(f)$ has also been included in the background of these plots for reference. The target values for θ_m and σ_θ are also shown by dashed lines on these plots. Although the theoretical spreading width is 31.7 deg. for test case P, the target σ_θ value has been set to 29.5 deg. which corresponds to truncating the theoretical spreading function at ± 70 degrees to comply with the minimum and maximum wave angles that can typically be generated at the test site in the various participating wave basins.

The various laboratory data sets generally show similar levels of variability with frequency. The accuracy of the (η, u, v) results tends to decrease somewhat with increasing frequency which may be due to increased noise in the current meter measurements at higher frequencies. Most of the results agree quite well with the target values on average. As noted previously, the Lab 3 waves were generated for a different target spreading of $\sigma_\theta = 21.6$ deg. as shown by the short dashed line in Figure 12d. The σ_θ results for Lab 3 are about 5 degrees less than their target value on average but otherwise have similar variability with frequency as the other results.

The corresponding $\theta_m(f)$ and $\sigma_\theta(f)$ results for test case Q are shown in Figure 13. In general, the variability with frequency is smaller than test case P over the main frequency range from 0.4 to 1.0 Hz. The variability of σ_θ for the 6-probe array data is somewhat larger, however. As before, the accuracy of the (η, u, v) results tends to decrease with increasing frequency. The 6-probe array σ_θ results for test case Q are about 3 degrees larger than the target value on average but all of the other test case Q results agree very well with the target values on average. The Lab 3 σ_θ results are about 4 deg. smaller than the other results on average which is consistent with the narrower target spreading that was used to generate these waves.

The $\theta_m(f)$ and $\sigma_\theta(f)$ results for test case R are shown in Figure 14. In general, these results are very similar to those for test case P, as shown in Figure 12. Thus, the increased wave steepness does not have a significant effect on these directional wave parameters.

7 Concluding Remarks

The following general observations can be made by comparing the numerical simulation results in Figures 7 and 8 with the corresponding results from the wave basin tests in Figures 12 and 13:

- The variability of $\theta_m(f)$ and $\sigma_\theta(f)$ is generally smaller for test case Q than for test case P for both the numerical simulations and the laboratory basin

- Bryden, I.G. and Greated, C.A., (1984): *Generation of three-dimensional random waves*, J. Phys. D: Appl. Phys., **17**, pp. 2351–2366.
- Cornett, A.M. et al. (1993): *Physical Modelling of Multidirectional Waves*, 2nd Int. Symposium on Ocean Wave Measurement and Analysis, New Orleans.
- Dalrymple, R.A., (1989): *Directional Wavemaker Theory with Sidewall Reflection*, Journal of Hydraulic Research, Vol. 27, No. 1, pp. 23–34.
- Gilbert, G. and Huntington, S.W., (1991): *A Technique for the Generation of Short Crested Waves in Wave Basins*, Journal of Hydraulic Research, Vol. 29, No. 6, pp. 789–799.
- Hawkes, P.J. et al., (1997): *Comparative Analyses of Multidirectional Wave Basin Data*, IAHR Seminar on Multidirectional Waves and their Interaction with Structures, XXVII IAHR Congress, San Francisco.
- Hiraishi, T. et al., (1992): *Validation of a Numerical Diffraction Model for Multidirectional Wave Generation*, Proc. 2nd Int. Offshore and Polar Eng. Conf., San Francisco, pp. 154–169.
- Isaacson, M. and Mathai, T., (1993): *Wave Field in a Laboratory Wave Basin with Partially Reflecting Boundaries*, Proc. 3rd Int. Offshore and Polar Eng. Conf., Singapore, pp. 669–676.
- Jefferys, E.R., (1987): *Directional Seas should be Ergodic*, Applied Ocean Research, **9**, (4), pp. 186–191.
- Miles, M.D., (1989): *A Note on Directional Random Wave Synthesis by the Single Summation Method*, Proc. XXIII IAHR Congress, Ottawa, pp. 243–250.
- Miles, M.D. and Funke, E.R., (1989): *A Comparison of Methods for Synthesis of Directional Seas*, ASME OMAE Journal, **111**, (1), pp. 43–48.
- Naeser, H., (1979): *Generation of Uniform Directional Spectra in a Wave Basin using the Natural Diffraction of Waves*, Proc. POAC, Norway, pp. 621–632.
- Nwogu, O.G., (1989): *Maximum Entropy Estimation of Directional Wave Spectra from an Array of Wave Probes*, Applied Ocean Research, **11**, 4, pp. 176–182.
- Nwogu, O.G., et al., (1987): *Estimation of Directional Wave Spectra by the Maximum Entropy Method*, IAHR Seminar on Wave Analysis and Generation in Laboratory Basins, XXII IAHR Congress, Lausanne, pp. 363–376.
- Sand, S.E., and Mynett, A.E., (1987): *Directional Wave Generation and Analysis*, IAHR Seminar on Wave Analysis and Generation in Laboratory Basins, XXII IAHR Congress, Lausanne, pp. 209–235.
- Suh, K. and Dalrymple, R.A., (1987): *Directional Wavemaker Theory: A Spectral Approach*, IAHR Seminar on Wave Analysis and Generation in Laboratory Basins, XXII IAHR Congress, Lausanne, pp. 389–395.

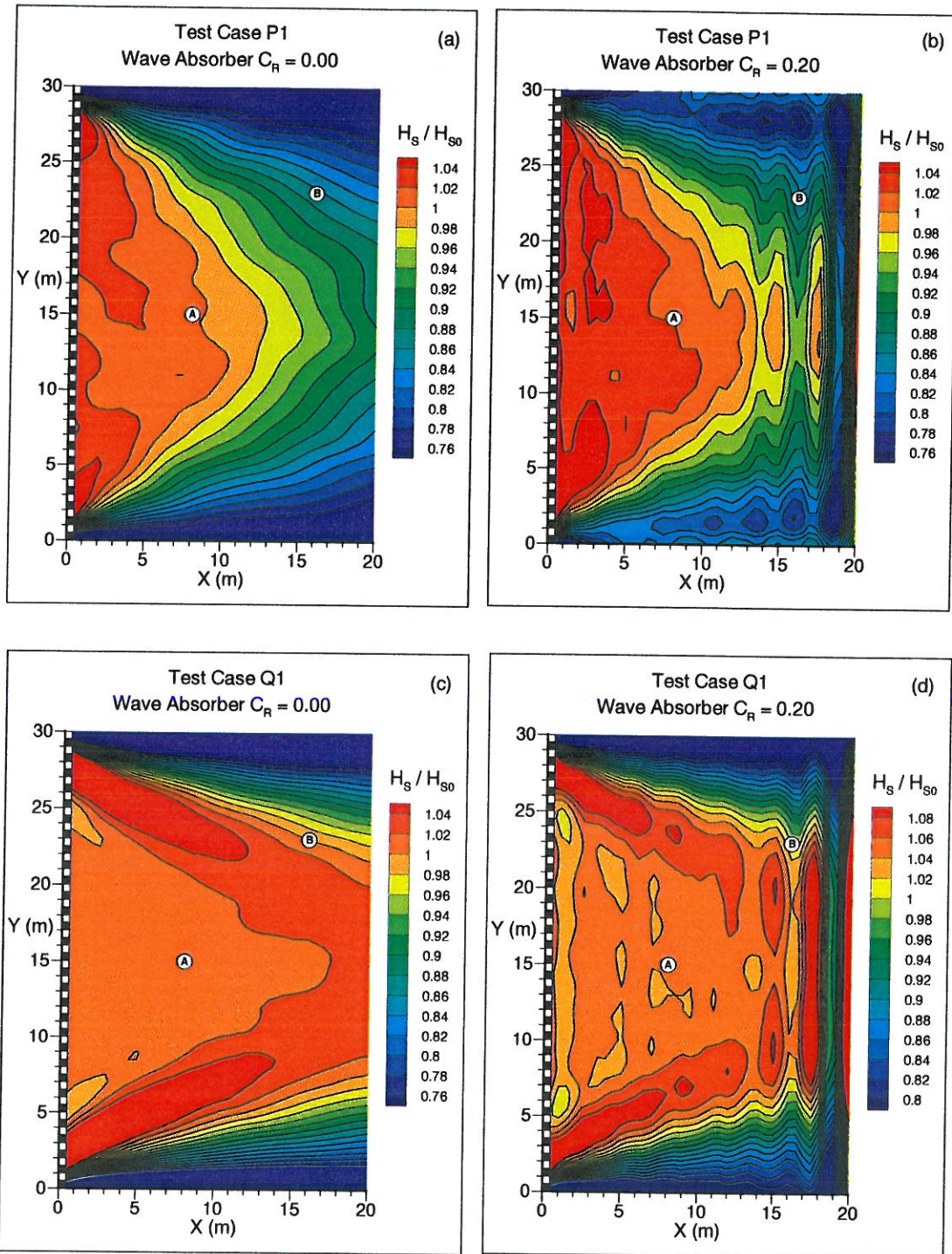


Figure 2: Normalized significant wave height from numerical simulations of Test Cases P1 and Q1

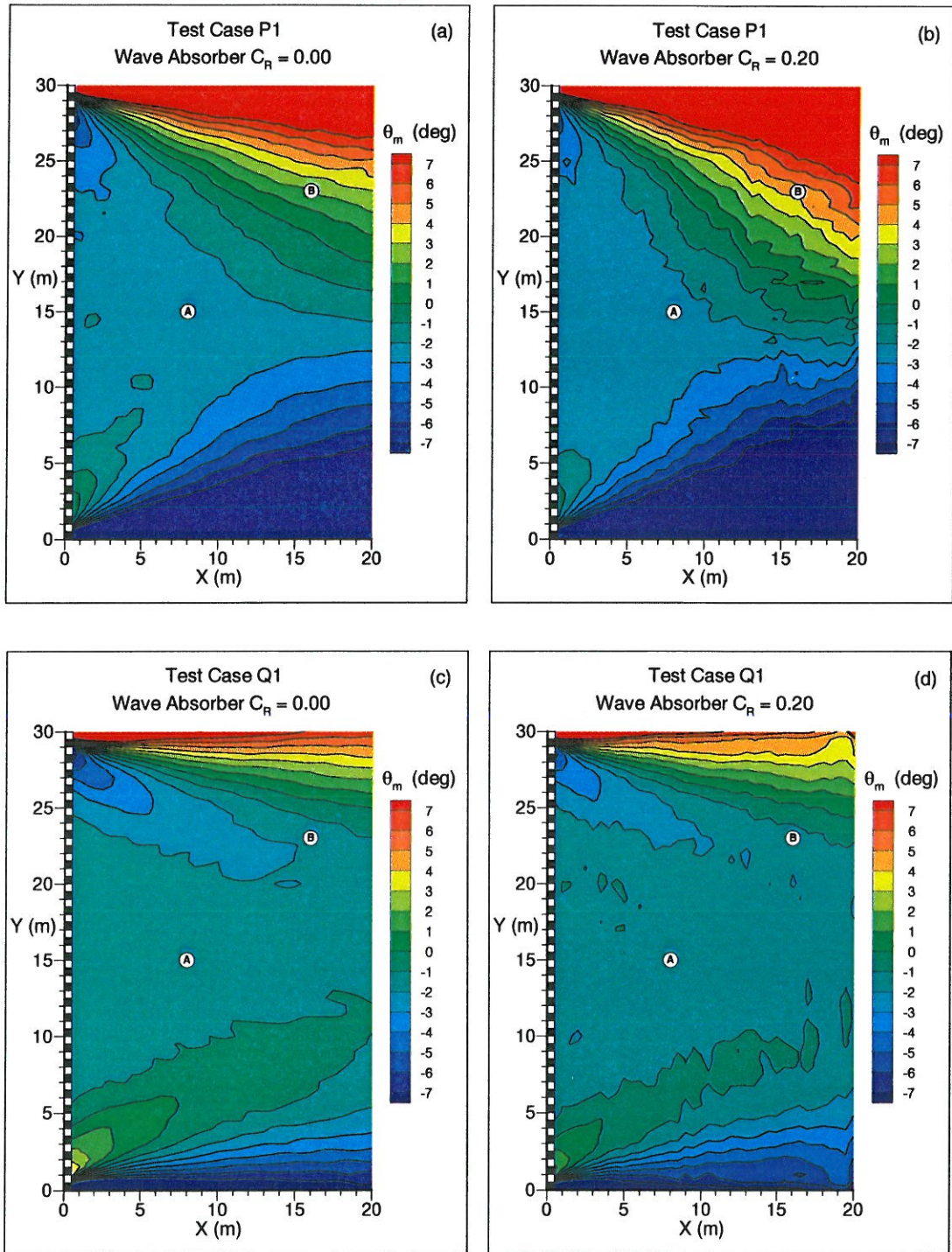


Figure 3: Mean wave direction θ_m for incident wave field from numerical simulations of Test Cases P1 and Q1

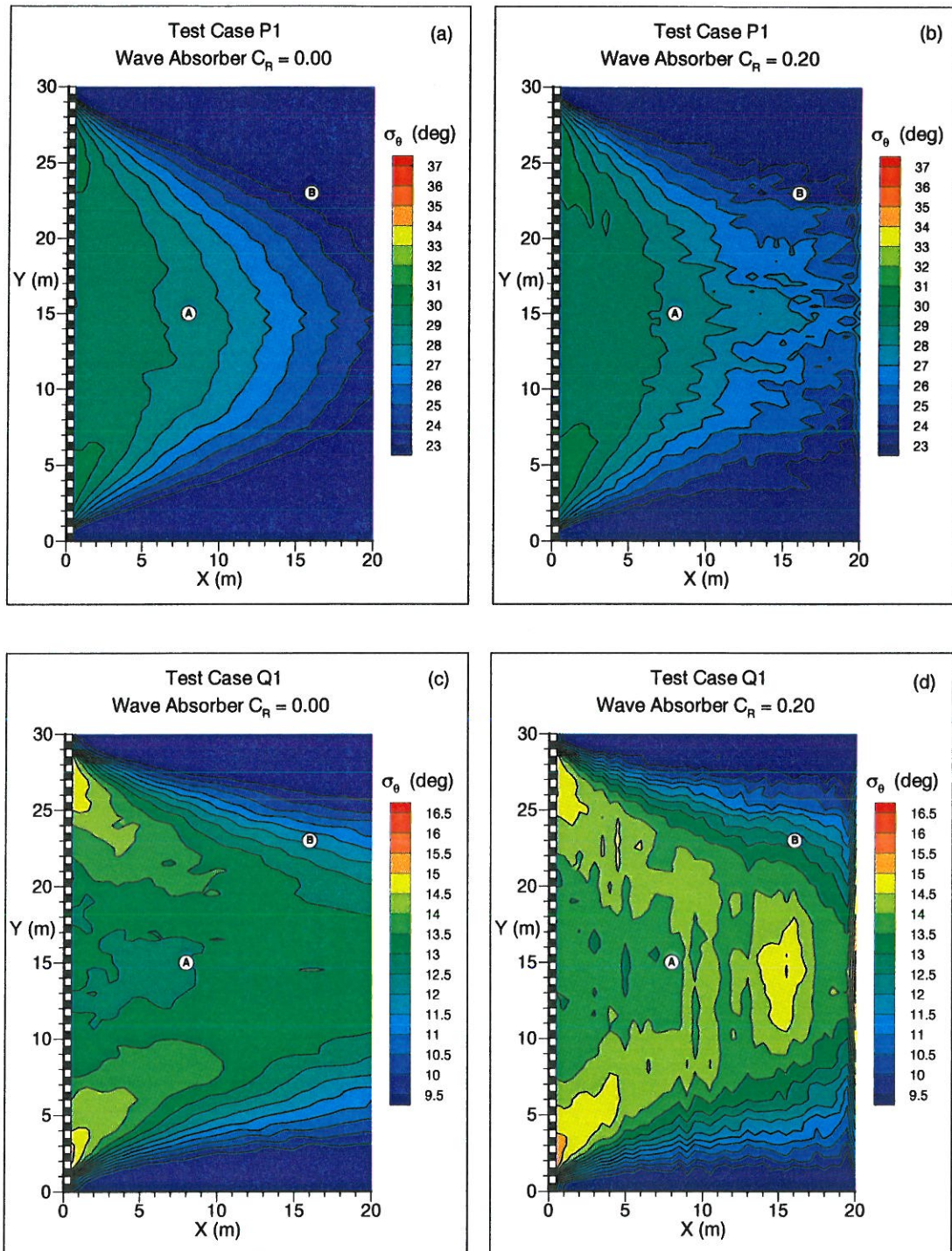


Figure 4: Spreading width σ_θ for incident wave field from numerical simulations of Test Cases P1 and Q1

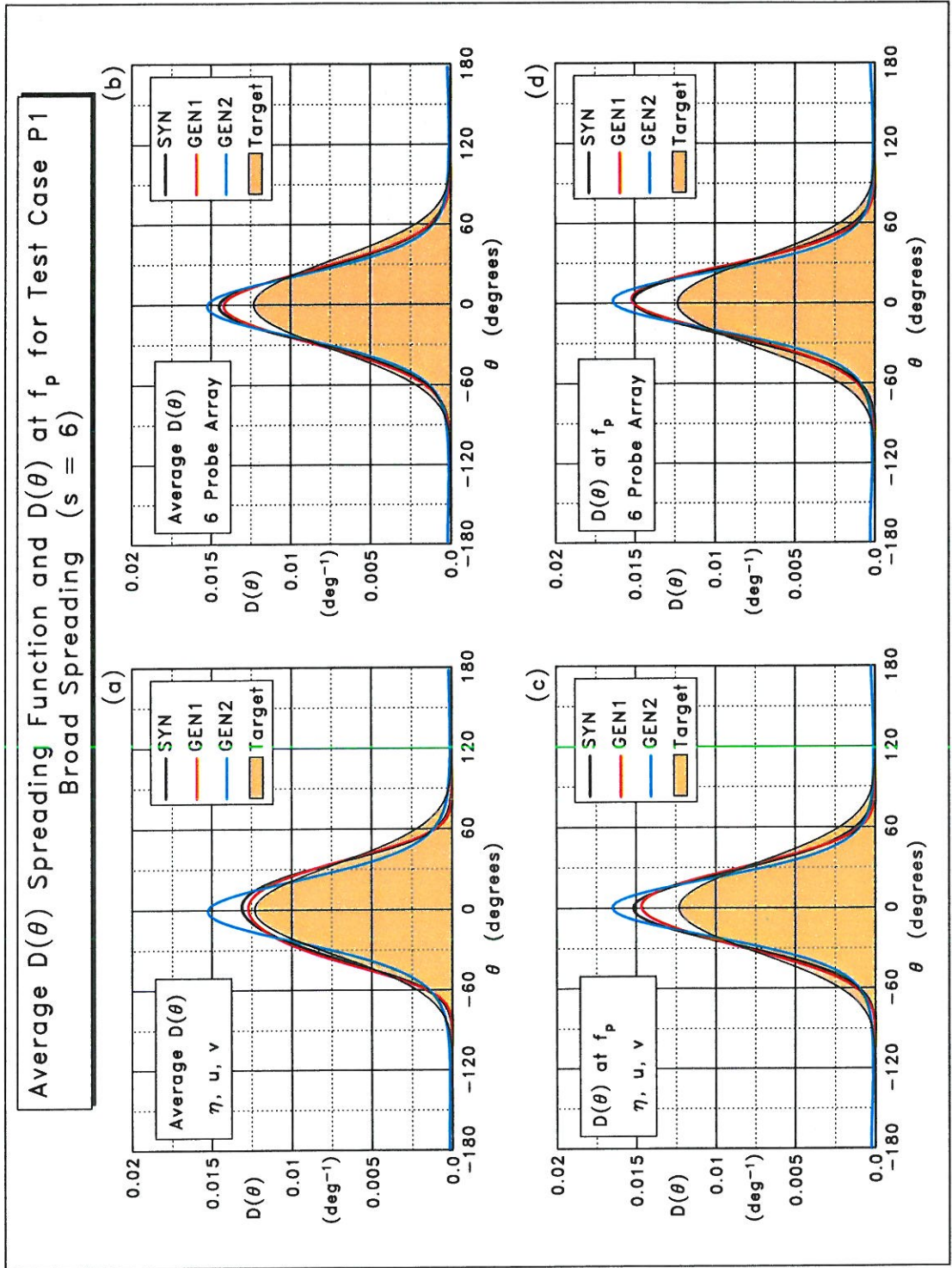


Figure 5: $D(\theta)$ spreading functions computed by programs MEMVL and MEMWP using time series data from numerical simulations of Test Case P1

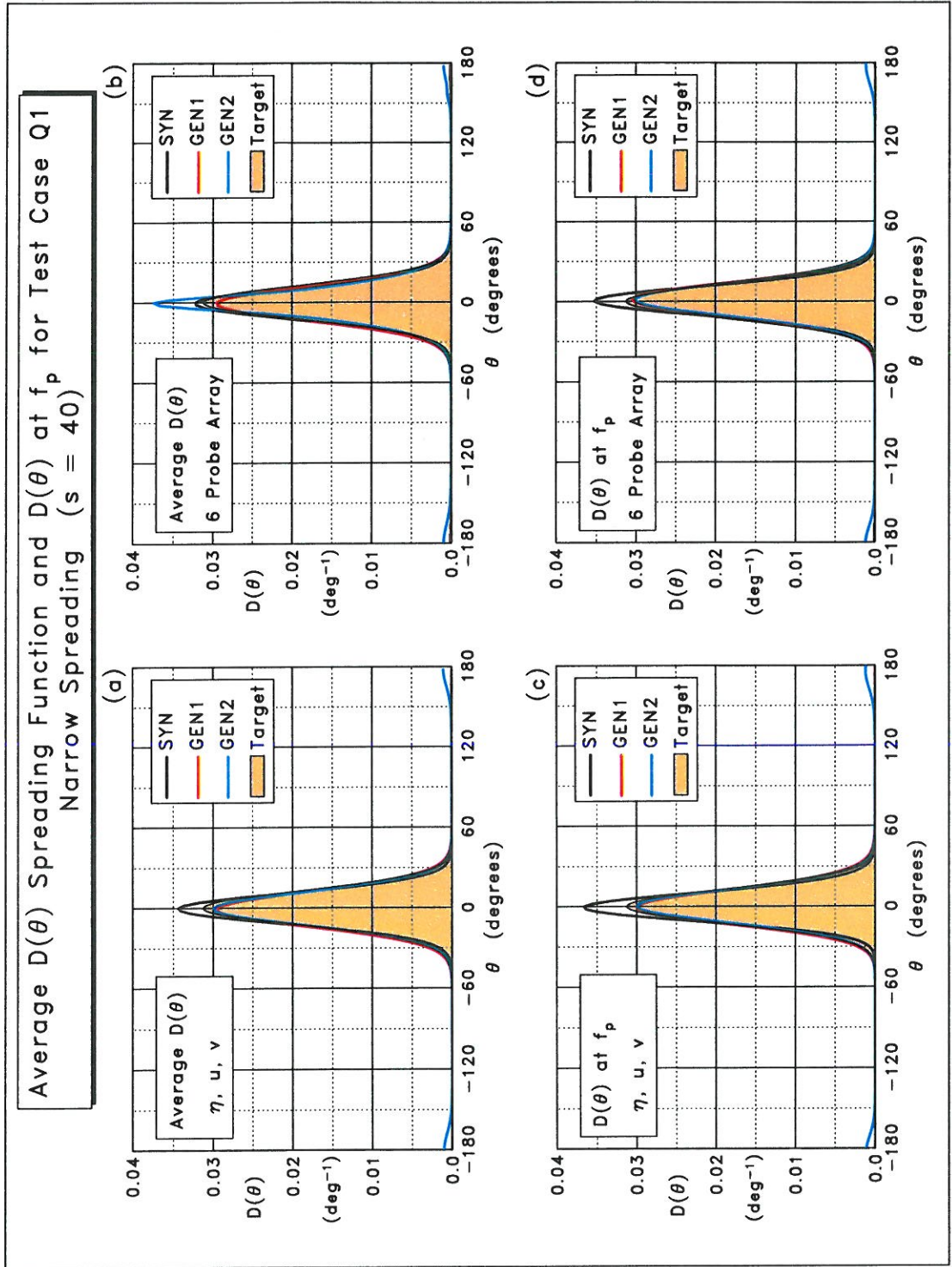


Figure 6: $D(\theta)$ spreading functions computed by programs MEMVL and MEMWP using time series data from numerical simulations of Test Case Q1

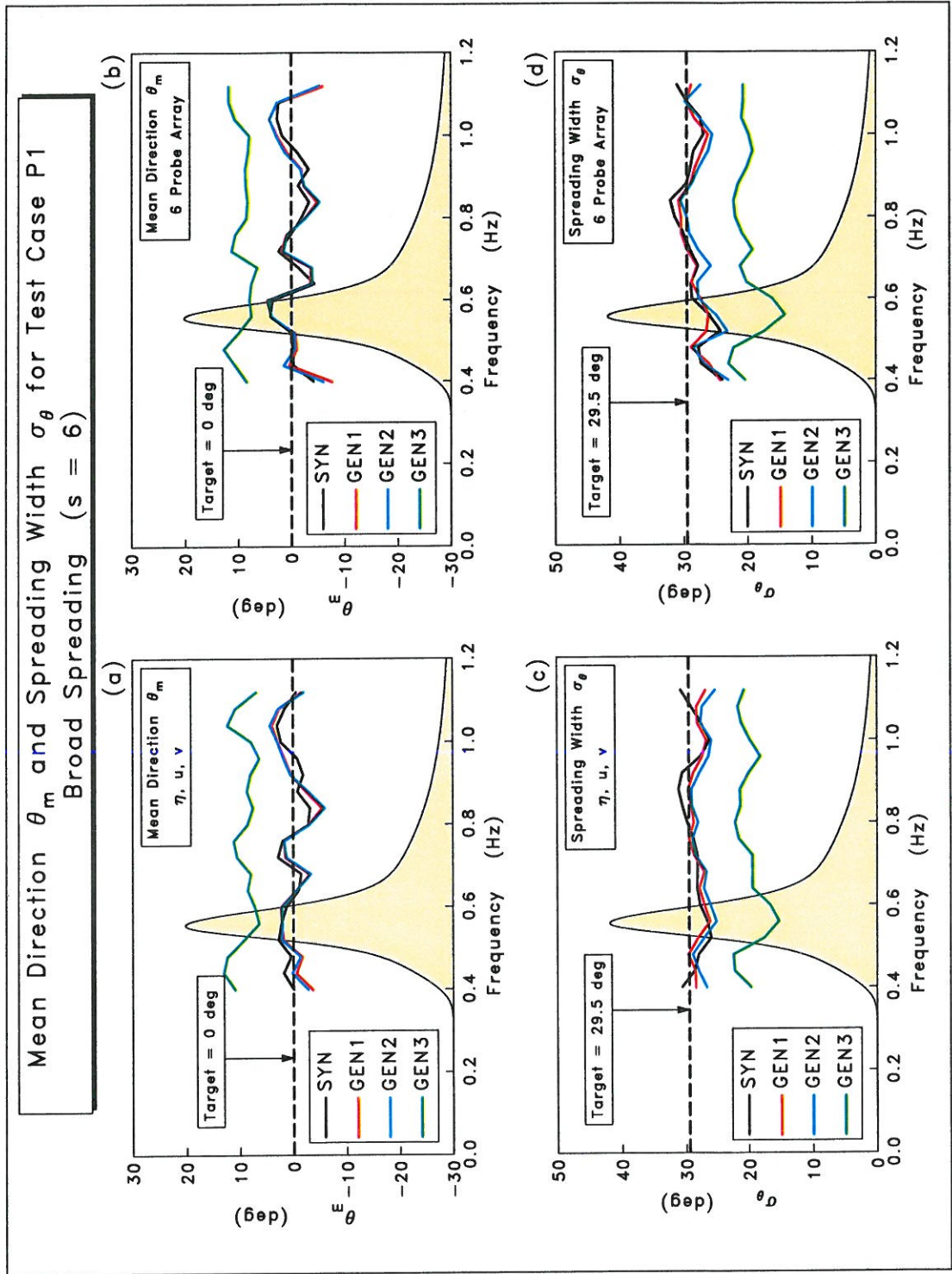


Figure 7: Mean wave direction $\theta_m(f)$ and spreading width $\sigma_\theta(f)$ computed by programs MEMVL and MEMWP using time series data from numerical simulations of Test Case P1

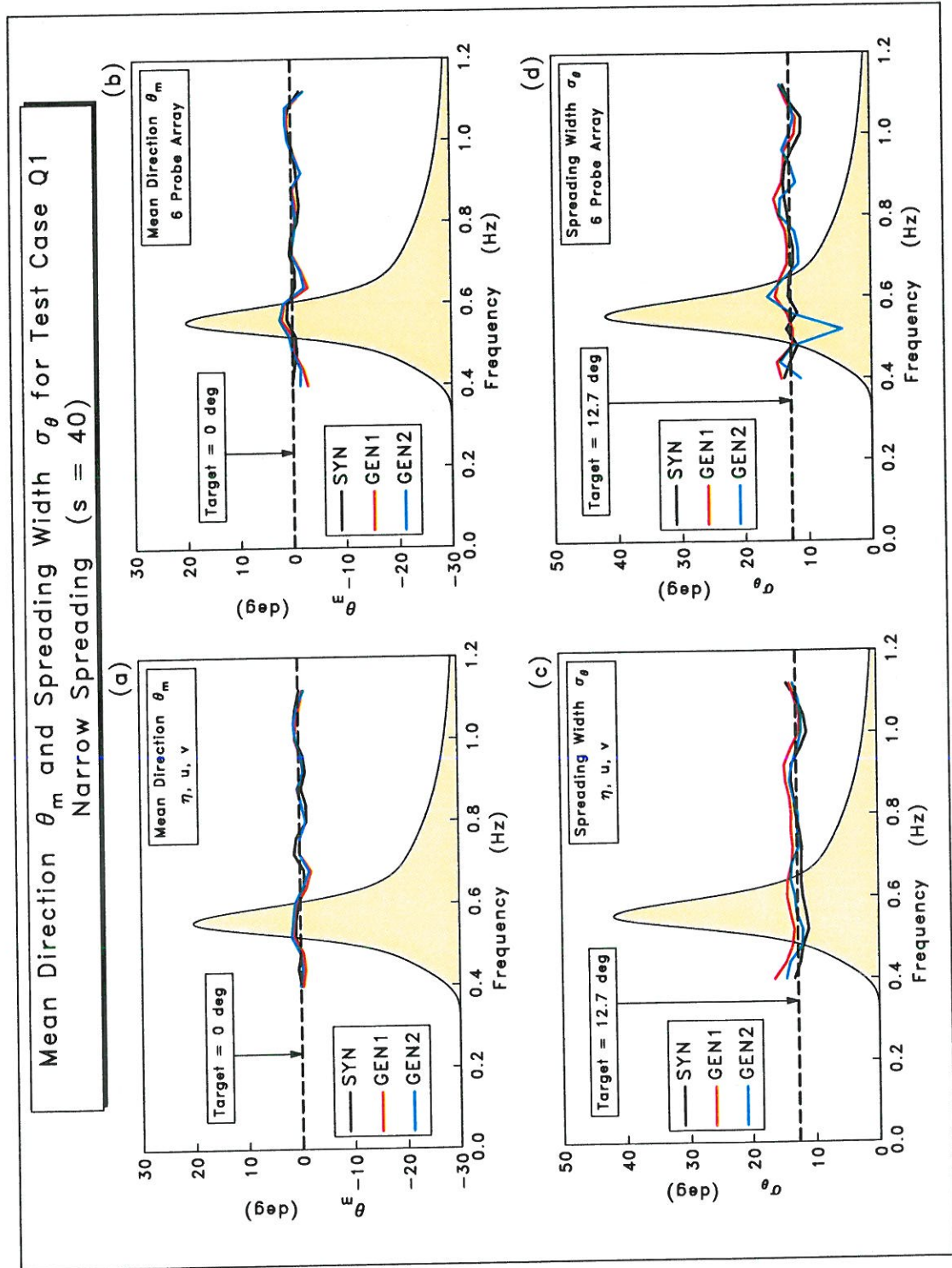


Figure 8: Mean wave direction $\theta_m(f)$ and spreading width $\sigma_\theta(f)$ computed by programs MEMVL and MEMWP using time series data from numerical simulations of Test Case Q1

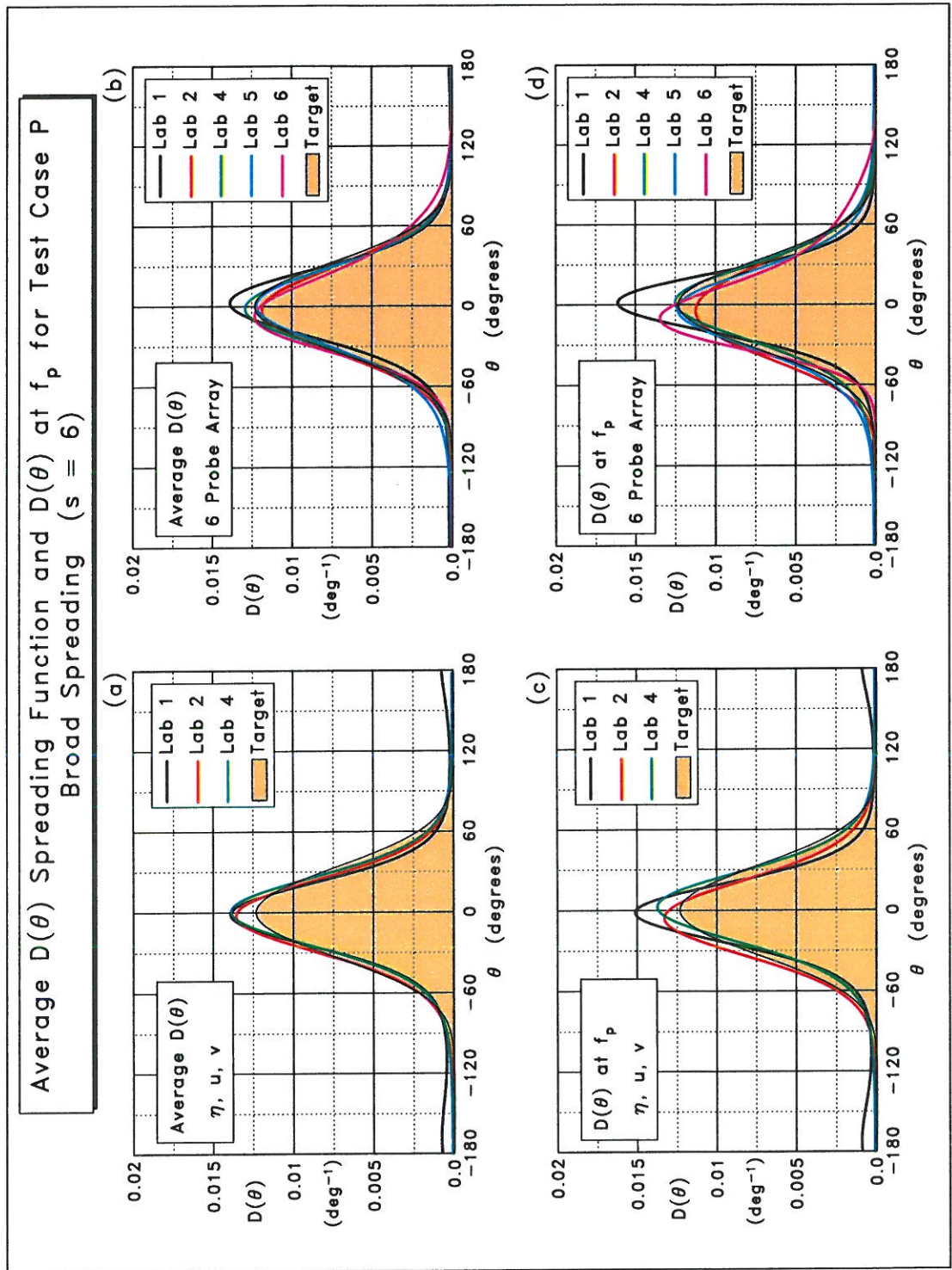


Figure 9: $D(\theta)$ spreading functions computed by programs MEMVL and MEMWP for waves generated in various laboratory basins for Test Case P

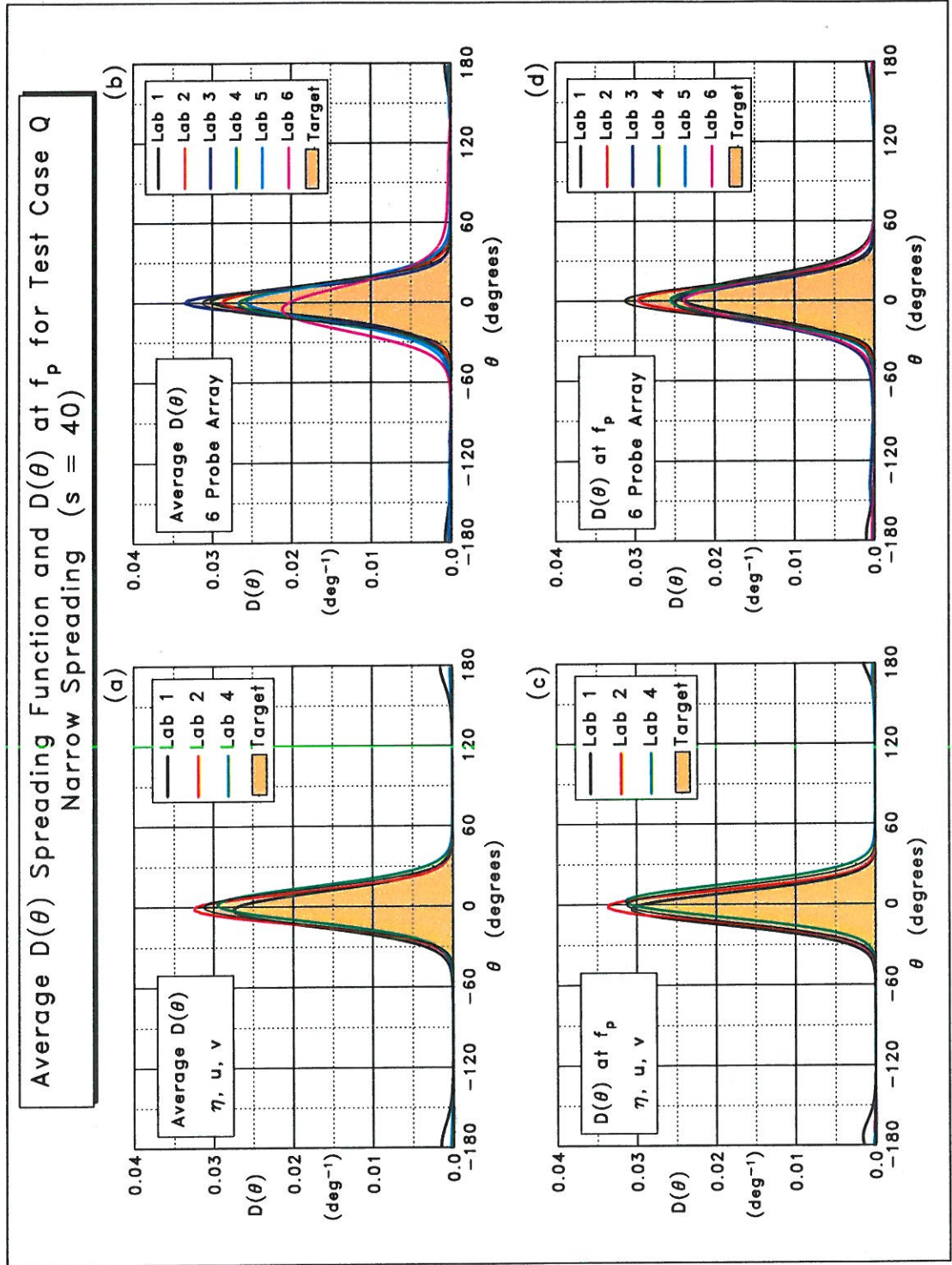


Figure 10: $D(\theta)$ spreading functions computed by programs MEMVL and MEMWP for waves generated in various laboratory basins for Test Case Q

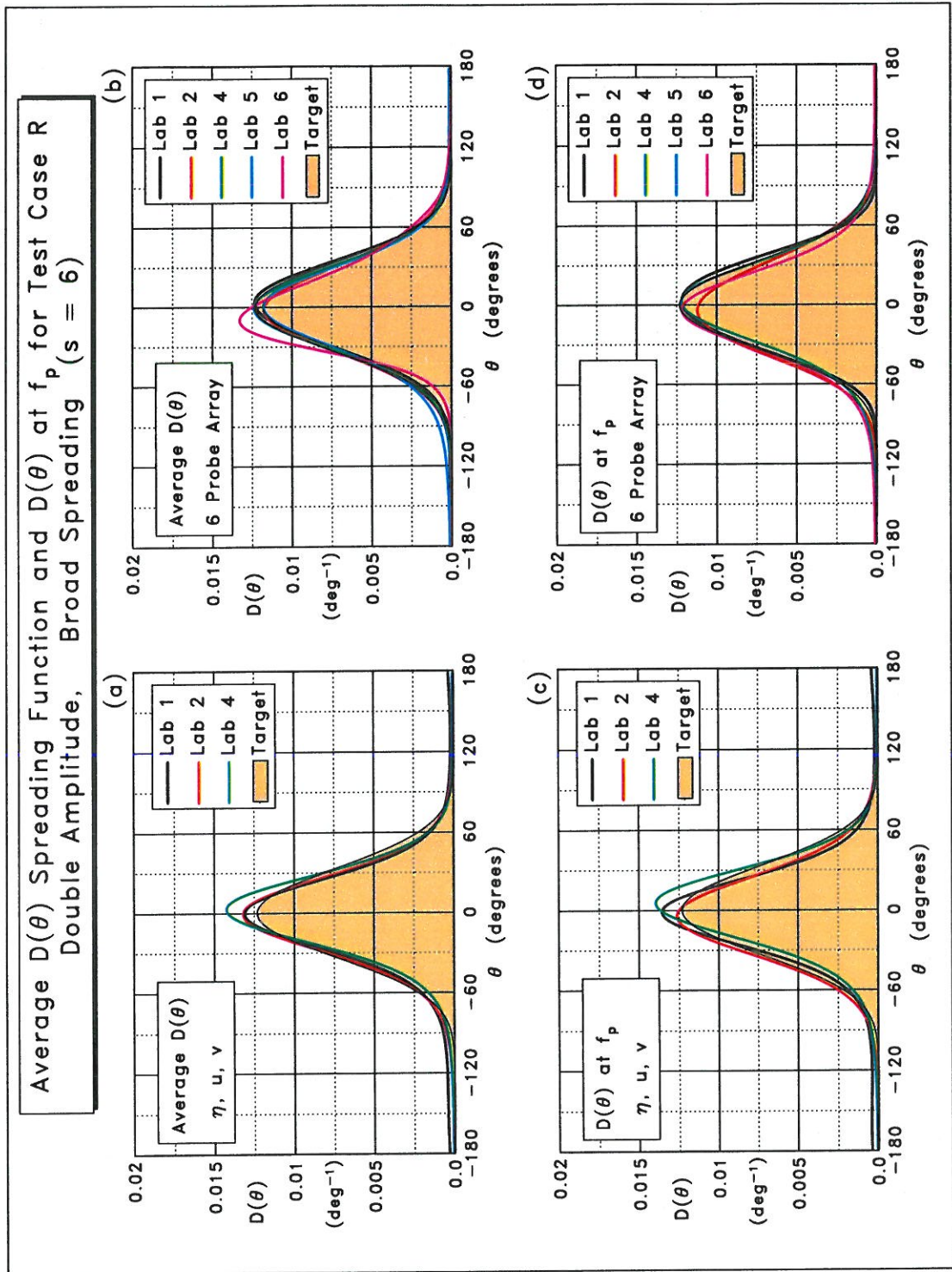


Figure 11: $D(\theta)$ spreading functions computed by programs MEMVL and MEMWP for waves generated in various laboratory basins for Test Case R

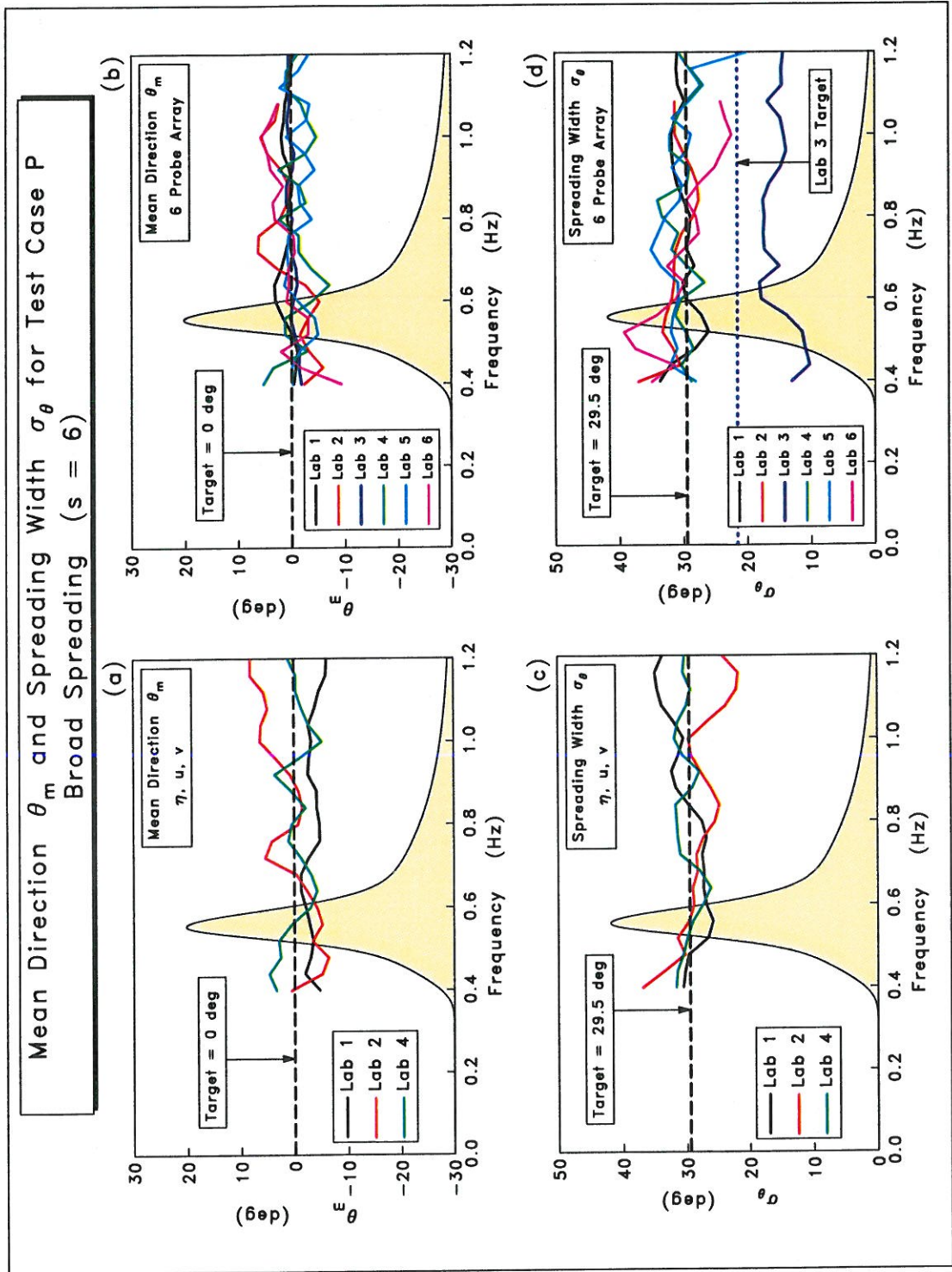


Figure 12: Mean wave direction $\theta_m(f)$ and spreading width $\sigma_\theta(f)$ computed by programs MEMVL and MEMWP for waves generated in various laboratory basins for Test Case P

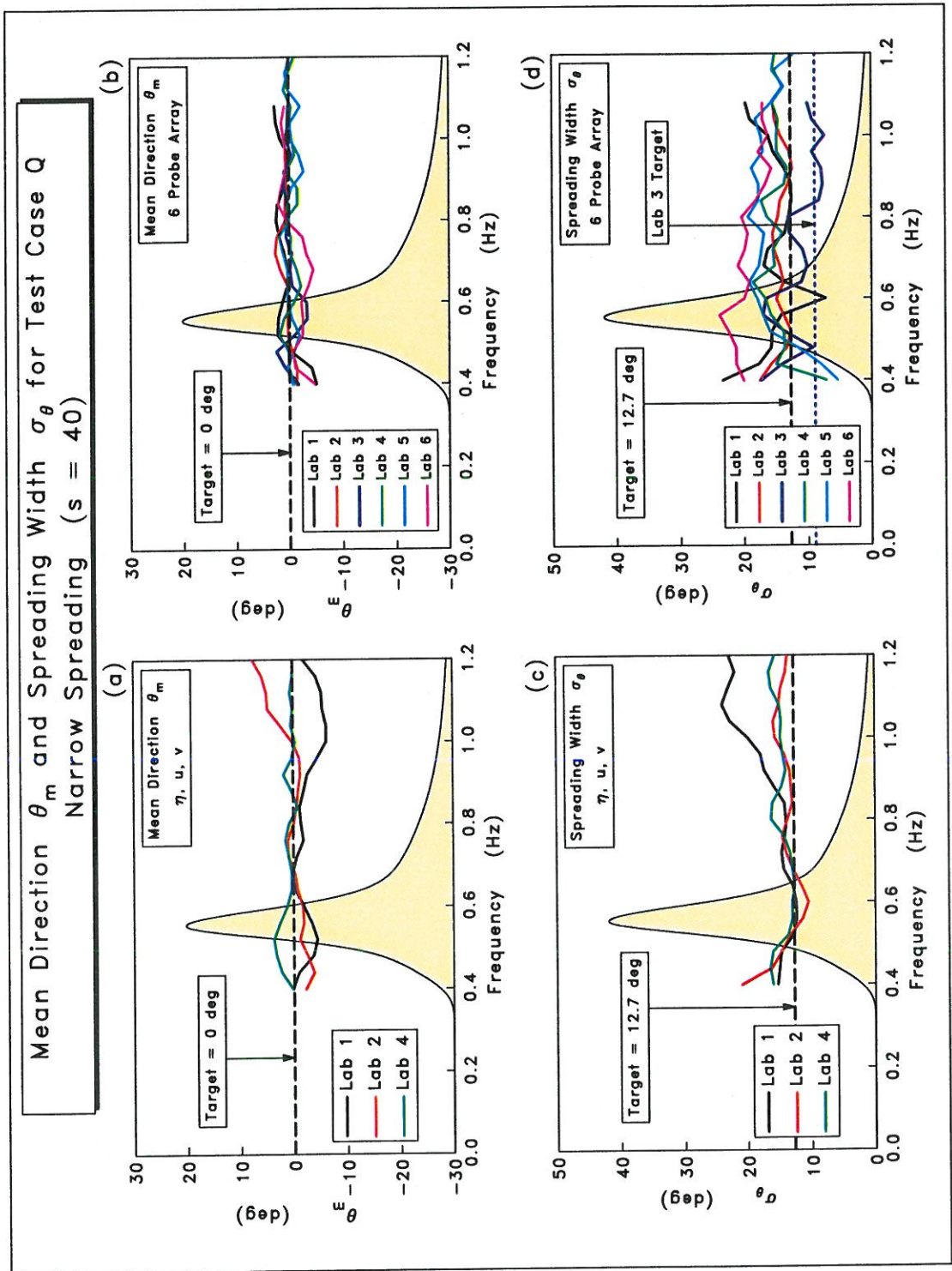


Figure 13: Mean wave direction $\theta_m(f)$ and spreading width $\sigma_\theta(f)$ computed by programs MEMVL and MEMWP for waves generated in various laboratory basins for Test Case Q

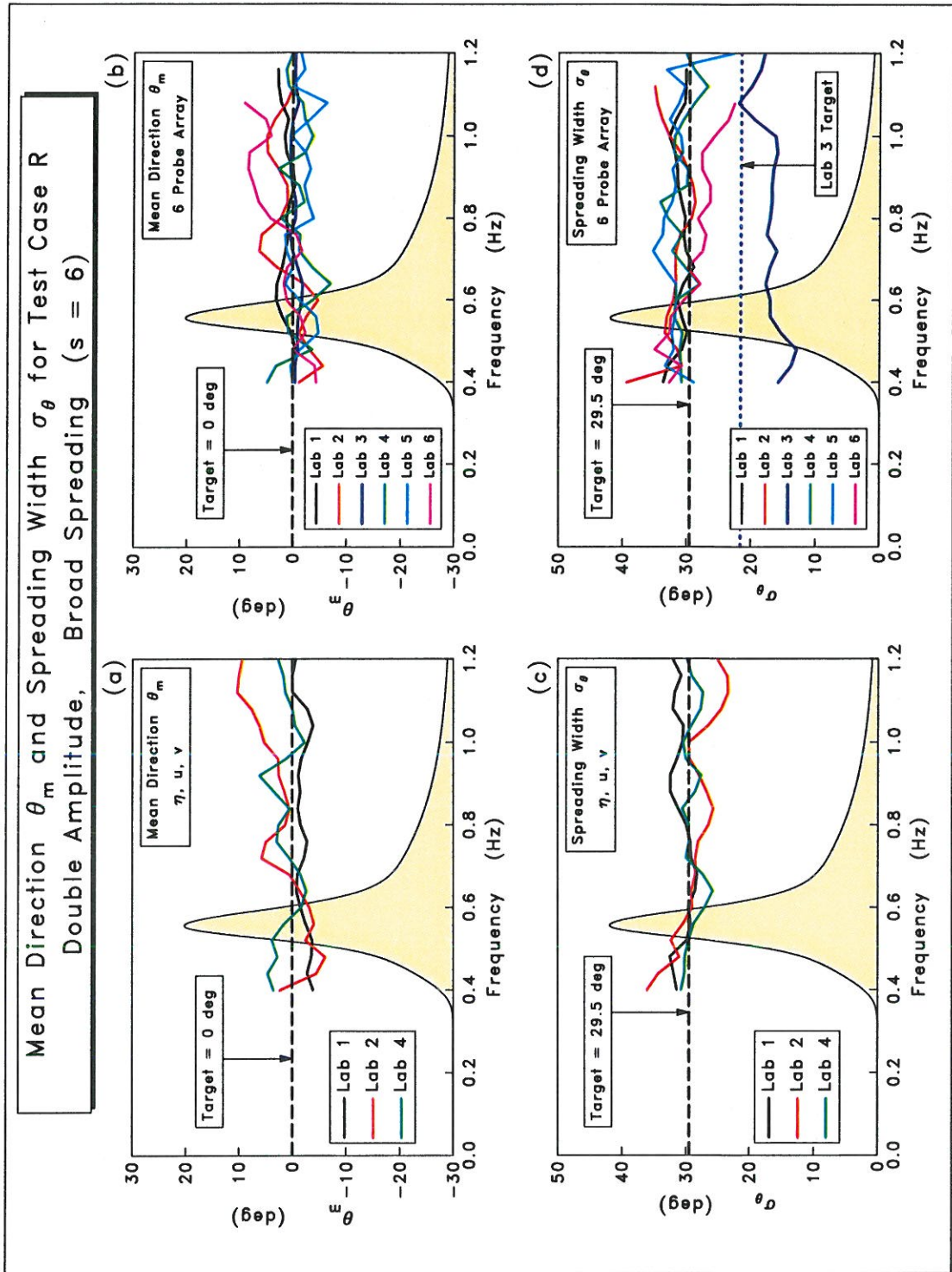


Figure 14: Mean wave direction $\theta_m(f)$ and spreading width $\sigma_\theta(f)$ computed by programs MEMVL and MEMWP for waves generated in various laboratory basins for Test Case R